

Direct-current-like phase space manipulation using chirped alternating current fields

P. F. Schmit and N. J. Fisch

Princeton Plasma Physics Laboratory, Princeton, New Jersey 08543, USA

(Received 2 June 2009; accepted 5 January 2010; published online 28 January 2010)

Waves in plasmas can accelerate particles that are resonant with the wave. A dc electric field also accelerates particles, but without a resonance discrimination, which makes the acceleration mechanism profoundly different. Whereas wave-particle acceleration mechanisms have been widely discussed in the literature, this work discusses the direct analogy between wave acceleration and dc field acceleration in a particular parameter regime explored in previous works. Apart from the academic interest of this correspondence, there may be practical advantages in using waves to mimic dc electric fields, for example, in driving plasma current with high efficiency.

© 2010 American Institute of Physics. [doi:[10.1063/1.3298860](https://doi.org/10.1063/1.3298860)]

I. INTRODUCTION

Accelerating waves can shift a particle distribution by a fixed displacement in velocity space, regardless of the initial configuration of the distribution, with a number of interesting applications.^{1–5} Filled and unfilled phase space holes can be used to accelerate particles for free electron laser applications: both by carrying filled buckets of phase space formed by chirped rf fields to higher energies, or by using empty buckets of virtual particles and displacing them through a distribution.^{3,4} In the case of free electron lasers,⁵ the phase space deceleration makes use of a ponderomotive hole in phase space accelerated through a beam to slow it down. Recently, an autoresonant mechanism, through self-consistent Bernstein, Green, and Kruskal (BGK) modes, was suggested to accelerate the full electron distribution, with applications to current drive as well.^{1,2} The idea of producing holes in phase space through BGK modes has been explored further both experimentally and theoretically.^{6–8}

There are of course in addition many specific wave mechanisms that have been advanced to manipulate a particle distribution in phase space, such as recently ponderomotive methods where particles exit a ponderomotive potential in an appropriate way,^{9–20} ratchet effects using a cyclotron resonance,^{21–23} and wakefield acceleration effects²⁴ including acceleration in plasma channels.²⁵

The particle dynamics underlying all of these applications is by now well researched. In particular, single degree-of-freedom Hamiltonians with slowly varying parameters have been considered in detail using formal Hamiltonian perturbation theory.^{26–28} While the dynamics are well understood, what is pointed out here is that waves can in fact mimic dc-like acceleration to arbitrarily small discrepancy: namely, each particle in the distribution receives an identical impulse independent of its initial conditions. In other words, a wave can produce an effect on a distribution of particles indistinguishable from that of a uniform dc field. The regime in which this occurs to arbitrarily small discrepancy is that in which the waves form an adiabatically (slowly) accelerating ponderomotive barrier. As the ponderomotive wave packets are accelerated through a distribution of particles, nearly all

particles receive the same impulse, except that by phase space conservation, some particles must be pushed ahead of the wave packet. However, the particles that are pushed ahead contain vanishingly small density, momentum, and energy in the limit of adiabatic acceleration. While this regime can be anticipated from the mathematical literature, the full correspondence to the dc limit has not yet been drawn.

We further propose here that it is of both academic and practical interest that ac fields can mimic dc fields perfectly in some limit. In particular, there is an interesting application to current drive techniques. These fields are fundamentally different: ac fields, or waves, penetrate plasma in ways that dc fields cannot. Yet dc fields can drive electric currents with much higher efficiency than ac fields, suggesting that dc-like current drive efficiencies might be achievable with ac fields.

Apart from the practical matter of current generation and other effects associated with dc fields, the fact that there is a limit in which ac fields perfectly mimic dc fields may be of further academic interest. There is possibly a deeper underlying principle at play in that the ponderomotive packets of waves, which are like particles, can produce dc force fields much in the same way that force carriers mediate force fields in quantum field theory.

Having pointed to the importance of the problem, we describe here the extent to which one can accelerate a full distribution of particles in a manner *identical* to a dc electric field using ac fields. It is of interest to show not only that each bit of phase space can be uniformly accelerated like a dc electric field would do, but also to describe how those regions of phase space that undergo further acceleration can be kept vanishingly small. Section II briefly reviews the acceleration of particles by waves in the particular regime of interest. Section III confirms the existence of the dc-like limit. Section IV compares driving currents with ac and dc fields and points out the importance of this mechanism as a potential means of current drive that incorporates advantages from both the ac and dc methods. The main effects uncovered here are summarized in Sec. V, and auxiliary calculations are presented in the Appendix for completeness.

II. BRIEF REVIEW OF ACCELERATION WITH ac FIELDS

To illustrate explicitly the limit in which ac fields can act as dc fields, consider a potential of the form

$$\Phi(x, t) = \Phi_0 \cos\{k[x - \Psi(t)]\}, \quad (1)$$

acting on an arbitrary one-dimensional distribution of noninteracting classical particles. This potential is similar to that used by Friedland *et al.*^{1,2} as well as by Shneider *et al.*⁹ to approximate the effects of an accelerating beat wave, or optical lattice, generated by two counterpropagating frequency-chirped electromagnetic waves. This potential can be formed by counterpropagating waves, say of the form $A_1 \sin(k_1 x + \omega_1 t)$ and $A_2 \sin(k_2 x + \omega_2 t)$, with ω_1/k_1 of the opposite sign of ω_2/k_2 . With an appropriate choice of parameters for each wave and time-averaging over the fast oscillations, one can obtain an average ponderomotive potential taking on the spatial profile of the envelope of the two sinusoidal waves [cf. the discussion following Eq. (16)]. Thus, by modulating the underlying frequencies of the two drive waves, it could be possible to vary the phase velocity of the envelope and create an accelerating one-dimensional potential like that in Eq. (1). This is a specific case of the more general one-dimensional time-dependent potentials studied by Chirikov, Cary, and Neishtadt.^{26–28} However, in order to show the dc limit it suffices to take the potential in this form rather than requiring self-consistent fields or including more complicated time dependencies.

The effect of the potential defined in Eq. (1) on a classical particle is illustrated in Fig. 1. Small fluctuations in the particle velocity become larger as wave-particle resonance is approached, at which point a resonance interaction occurs. Afterward, the large fluctuations decay and the particle is left with a net impulse. For adiabatic acceleration, the acceleration is small enough so that for most of the duration of the interaction the change in the wave phase velocity during the time it takes the particle to traverse one period of the wave is small compared with the relative velocity between the particle and the wave, v_{rel} , or in other words,

$$\frac{2\pi a}{kv_{\text{rel}} v_{\text{rel}}} \sim \frac{a}{kv_{\text{rel}}^2} \ll 1. \quad (2)$$

In the limit of adiabatic acceleration of the waveform, the wave phase velocity $\dot{\Psi}$ remains approximately constant over time scales comparable to $2\pi/kv_{\text{rel}}$, the particle transit time in the wave. On this time scale, all instantaneous phase space trajectories are given by the equation

$$\dot{x}_{\pm}(t) = \dot{\Psi}(t) \pm \left[\frac{2\Phi_0}{m} (\alpha - \cos\{k[x - \Psi(t)]\}) \right]^{1/2}, \quad (3)$$

where

$$\alpha \equiv \frac{1}{\Phi_0} [1/2m(\dot{x} - \dot{\Psi})^2 + \Phi_0 \cos\{k(x - \Psi)\}] \quad (4)$$

is an approximately conserved quantity on this time scale and represents the ratio of the energy of a particle in the rest frame of the wave to the maximum strength of the potential. Orbits with $\alpha > 1$ are topologically open, orbits with $\alpha < 1$

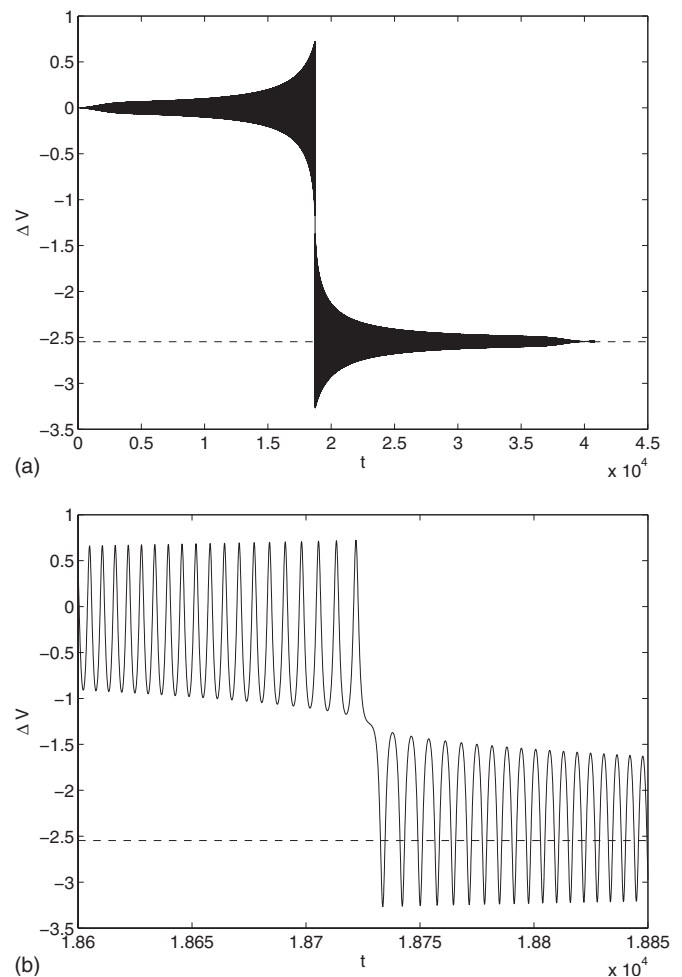


FIG. 1. (a) Net impulse delivered to initially stationary particle at the origin in the laboratory reference frame vs time. (b) Close-up of impulse vs time near the resonance. The dotted line shows predicted Δx according to time-asymptotic conservation of action, cf. Eq. (7).

are topologically closed, and the orbit given by $\alpha=1$ defines the separatrix dividing phase space into regions of purely untrapped versus purely trapped orbits. An example snapshot of the various phase space trajectories for transit-time scales is depicted in Fig. 2. Notice that trajectories for particles traveling at a velocity substantially different from the instantaneous velocity of the waveform, i.e., $\alpha \gg 1$, can be represented as approximately straight, fixed-velocity lines, since they are far out of resonance with the wave and hence barely feel its effects.

Envision a particle distribution extending infinitely in one-dimensional configuration space but only across a finite range of velocity space, forming what is often called a “waterbag” distribution. When the wave is far out of resonance with the distribution, the waterbag is approximately unchanged in time. Thus all particle orbits are open, and the trapped-particle states confined within the wave’s separatrices start out unpopulated. Because the wave is adiabatically accelerated, the trapped particle states remain essentially inaccessible to particles in the distribution, which all began on open orbits.

Now consider the situation where the wave has resonantly interacted with one velocity-space boundary of the

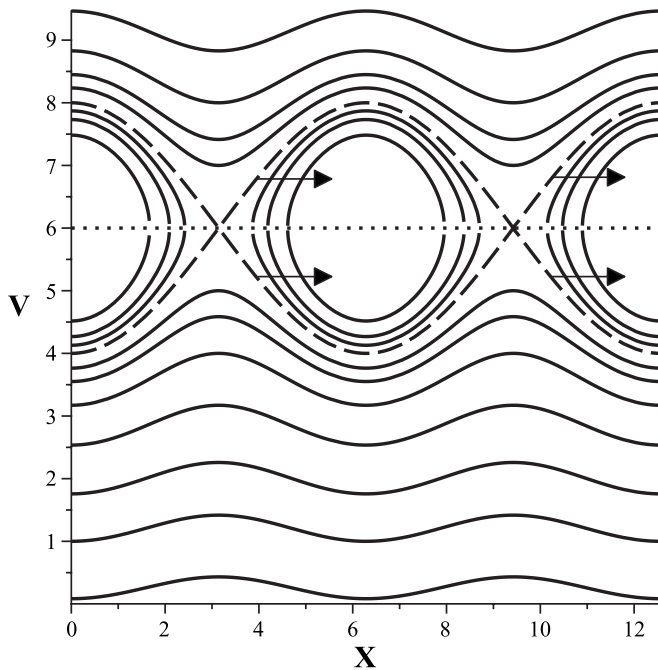


FIG. 2. Snapshot of phase space trajectories during transit-time scales, for which $\dot{\Psi} \approx \text{const}$. Separatrices are denoted by dashed line, instantaneous wave phase velocity $\dot{\Psi}$ is denoted by the dotted line, and the direction of translation of the orbits is indicated by arrows.

distribution such that the separatrices now lie in the middle of the distribution. Resonance between the wave and a particle occupying the boundary is described in Fig. 3. Because the waveform acceleration is presumed to be adiabatic, the closed-orbit trajectories remain unpopulated and the separatrices form the boundaries of empty holes inside the distribution. If the edges of the distribution in velocity space are far enough apart that neither is resonantly interacting with the wave, then they will both have the approximate asymptotic form of a straight line. Only the boundary of the distribution through which the separatrices came can be changed from the original picture, while the other boundary has yet to resonantly interact with the waveform. By Liouville's theorem, the phase space volume of the distribution

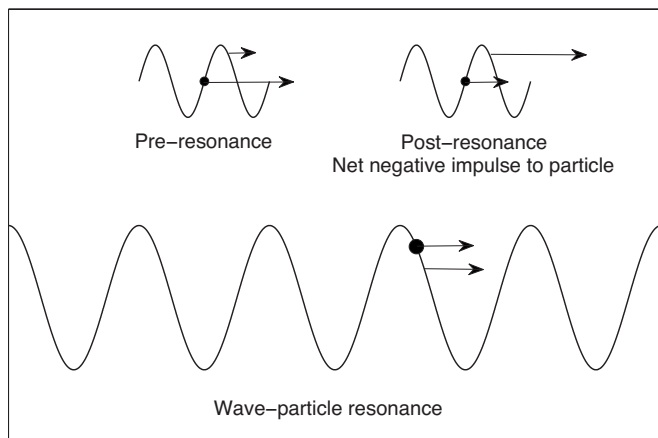


FIG. 3. Graphic illustrating the different stages of the wave-particle interaction: preresonance, resonance, and postresonance.

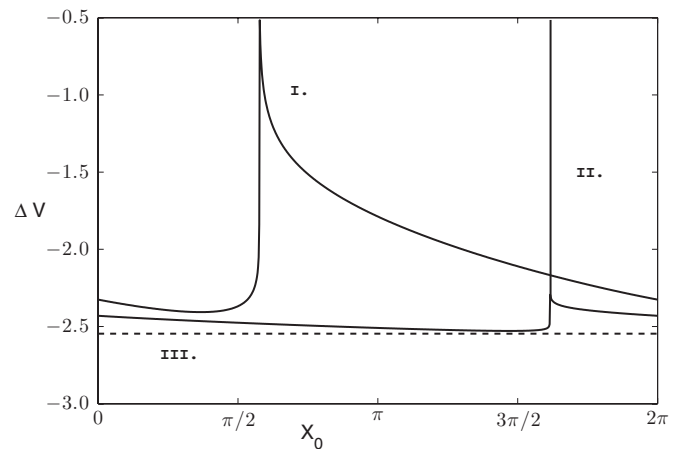


FIG. 4. Numerical simulations show the time-asymptotic impulse delivered to one period of the initial distribution for I, $\epsilon = 10^{-1}$ and II, $\epsilon = 10^{-2}$, cf. Eq. (9). Line III shows the conserved action prediction for the impulse from Eq. (7).

must be preserved, and so the boundary that has already resonantly interacted with the wave must be displaced in order to account for the empty volume inserted into the distribution by the empty trapped-particle states. The action, or phase space volume $\int p dq$, per unit wavelength $\lambda = 2\pi/k$ of a straight line, which describes the nonresonantly interacting boundaries of the distribution, is given simply by $J_{sl} = \lambda m \dot{x}$, while the phase space volume of the separatrices is found to be

$$J_{sep} = \left[m \int_0^\lambda (\dot{x}_+ - \dot{x}_-) dx \right]_{\alpha=1} = 16 \frac{\sqrt{m\Phi_0}}{k} \tag{5}$$

[cf. Eq. (3)]. Liouville's theorem can be stated as a jump condition

$$J_{sl,f} = J_{sl,i} + J_{sep}, \tag{6}$$

yielding the final result for the distribution boundary,

$$|\Delta \dot{x}| = \frac{8}{\pi} \sqrt{\frac{\Phi_0}{m}}, \tag{7}$$

with the direction of the impulse opposite the direction of acceleration of the wave phase velocity. Similar arguments suggest that the trailing boundary undergoes a shift in velocity space identical to the shift of the leading boundary following resonance, leaving another waterbag distribution displaced in velocity space. This is the result stated by Friedland *et al.*,^{1,2} and it led to their suggestion that this phenomenon could be used as a viable current drive scheme in plasmas.

However, a uniform acceleration appears to violate the continuity of the solution with respect to initial conditions, since some particles must be accelerated ahead of the wave in order to maintain continuity. Numerical simulations show the formation of tendrils of the distribution that are carried away with the wave separatrices, opposite to the direction of the adiabatic impulse, cf. Fig. 4. No matter how slow the acceleration, these highly resonant tendrils never appear to vanish completely.

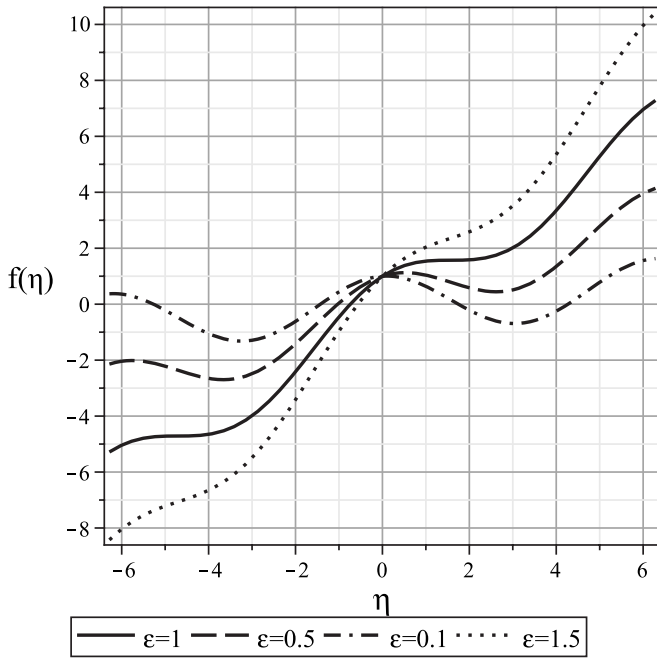


FIG. 5. Quasipotential in dynamic variable η plotted for $\bar{\phi}=1$ and several values of ϵ , cf. Eq. (10).

However, it can be shown that these tendrils become negligible as the wave acceleration becomes increasingly slow. Rewrite the nonlinear equation of motion for a particle in the potential given by Eq. (1) in terms of a dimensionless phase variable $\eta \equiv k[x - \Psi(t)]$,

$$\ddot{\eta} = \bar{\phi}[\sin \eta - \epsilon] = -\frac{df}{d\eta}, \tag{8}$$

with

$$\bar{\phi} \equiv a_{\text{crit}}k, \quad \epsilon \equiv a/a_{\text{crit}}, \quad a_{\text{crit}} \equiv \frac{\Phi_0 k}{m}, \tag{9}$$

where we have assumed, for simplicity, that the rate of acceleration is some constant a , i.e., $\Psi(t) = \frac{1}{2}at^2 + v_0t + x_0$. There exists a static quasipotential with an added linear term in this reference frame, and it is given by

$$f(\eta) = \bar{\phi}(\cos \eta + \epsilon\eta). \tag{10}$$

This quasipotential is plotted for $\bar{\phi}=1$ and several values of ϵ in Fig. 5.

Notice in Fig. 5 that any time the wave is accelerated such that $\epsilon \leq 1$, points of unstable equilibrium arise in the quasipotential, i.e., $df/d\eta=0$ and $d^2f/d\eta^2 < 0$, representing energies for which particles will resonantly interact with the wave for as long as the wave exists. These particles are connected to the bulk distribution by the continuous tendrils of phase space observed in Fig. 4. The particles in these tendrils lessen the efficiency of the uniform bucket displacement calculated in the zeroth order picture, cf. Eq. (7).

Using a method carried out in the Appendix, the impulse delivered to an arbitrary particle can be shown to scale approximately as

$$\Delta \dot{x}(\eta_t) \sim \frac{2\epsilon\bar{\phi}^{1/2}}{k} \left\{ \frac{\ln[1 + \Theta G + (\Theta^2 G^2 + 2\Theta G)^{1/2}]}{(\cos \eta_t)^{1/2}} + \frac{1}{\gamma^{1/2}} \tan^{-1} \left[\frac{(\gamma/2)^{1/2} \Theta}{[M - \gamma/2]^{1/2}} \right] - \frac{(2M)^{1/2}}{\epsilon} \right\}, \tag{11}$$

with

$$\Theta(\eta_t) = \frac{\eta_t - \eta_{\text{min}}}{2}, \quad \gamma = (1 - \epsilon^2)^{1/2},$$

$$G(\eta_t) = \frac{\cos \eta_t}{\epsilon - \sin \eta_t},$$

$$M(\eta_t) = \cos \eta_t + \epsilon \eta_t + \gamma + \epsilon(\pi + \sin^{-1} \epsilon),$$

and the variable η_t is the phase value corresponding to the particle's classical turning point in the quasipotential given by Eq. (10) and η_{min} is defined after Eq. (A7) in the Appendix. As is shown in the Appendix, η_t is constrained to values with $\eta_t \ll 1$ whenever $\epsilon \ll 1$, so Eq. (11) can be expanded for small ϵ and small η_t , and it takes the form

$$\Delta \dot{x} \sim \frac{2\epsilon\bar{\phi}^{1/2}}{k} \left[\ln \left(\frac{\pi}{\epsilon - \eta_t} \right) + \tan^{-1} \frac{\pi}{2\sqrt{3}} - \frac{2}{\epsilon} - \frac{\pi}{2} \right]. \tag{12}$$

Taking the limit as $\epsilon \rightarrow 0$, only one term survives,

$$\lim_{\epsilon \rightarrow 0} \Delta \dot{x} \sim -\frac{4\bar{\phi}^{1/2}}{k} = -4 \left(\frac{\Phi_0}{m} \right)^{1/2}, \tag{13}$$

where Eq. (9) was used to get to the final representation. Note that Eq. (13) predicts the same scaling as that demonstrated in Eq. (7).

III. THE EFFECTIVE dc LIMIT

Consider now the validity of the derivation of Eq. (13) for the case when η_t is very near ϵ ; in fact, when $\eta_t = \epsilon$ the impulse is infinite, which was the result of the particle coming to rest on the point of unstable equilibrium in the quasipotential. To see that the derivation remains valid, consider the case $\eta_t = \epsilon - \delta$ and $\delta = \epsilon^\alpha$, so that the following holds:

$$\epsilon \ln \left(\frac{1}{\epsilon - \eta_t} \right) = \epsilon \ln \left(\frac{1}{\delta} \right) = \alpha \epsilon \ln \left(\frac{1}{\epsilon} \right).$$

For any finite value of α the above expression goes to zero as $\epsilon \rightarrow 0$, which means no matter how close the particle comes to the singularity at $\eta_t = \epsilon$, the impulse will always be the adiabatic result shown in Eq. (13). Consequently, the density, momentum, and energy content of the tendrils of the distribution go to zero as the wave acceleration goes to zero, since a particle would have to have an exact initial energy corresponding to $\eta_t = 2\pi m + \arcsin \epsilon$ to get caught in the tendril, and any infinitesimal fluctuation away from that energy would immediately shift it to the adiabatically displaced bulk.

Thus as a classical wave is adiabatically accelerated through resonance with a noninteracting Hamiltonian distribution of particles at a rate that becomes infinitely slow, its time-asymptotic effect on the distribution becomes indistin-

guishable from the effect of a uniform dc field applied for a finite amount of time; namely, the impulse delivered to each particle is independent of the particle's initial conditions in phase space.

In the following the results of Sec. II, encapsulated in Eqs. (7), (11), and (13), are shown to be in agreement with previous calculations of the impulse by Chirikov, Cary, and Neishtadt.^{26–28} Chirikov's work with general fixed amplitude, variable phase velocity, one-dimensional sinusoidal potentials²⁶ and Cary and Neishtadt's later work with variable amplitude, variable phase velocity, one-dimensional potentials^{27,28} using Hamiltonian time-dependent perturbation theory similarly show the singularities in $\Delta\dot{x}$ to be logarithmic in the small parameters describing the temporal evolution of the potential. In Eq. (84) of their article, Cary *et al.* refine Chirikov's initial calculation of the change in mean momentum, denoted by $\Delta\bar{p}$ and defined as the action integral over one oscillation period divided by $2\pi m^{1/2}$, of a particle in a fixed-amplitude sinusoidal potential accelerating with arbitrary but slow acceleration. Cary's result is stated in terms of a parameter h_0 , which is defined as the particle energy at the coordinate of the separatrix X-point at the part of the trajectory nearest the separatrix crossing, calculated in the reference frame where the X-point is stationary. In terms of η_i , $h_0 = \Phi_0[\cos \eta_i + \epsilon(2\pi + \eta_i) - 1] \approx \Phi_0[\epsilon(2\pi + \eta_i) - \eta_i^2/2]$. Plugging in the values for h_0 and all other appropriate parameters, it is found that similar to the peak resonant impulse calculated here, which is a different physical quantity than $\Delta\bar{p}$, the change in average velocity $\Delta\bar{x} = (\Phi_0/m)^{1/2}[-8/\pi + \mathcal{O}(\alpha \ln \alpha)]$, with $\alpha = h_0/\Phi_0 \sim \epsilon$ to lowest order in ϵ . The zeroth order change matches the prediction from the bucket displacement picture, Eq. (7), while the next order terms demonstrate a similar kind of logarithmic scaling as the calculation of the peak resonant impulse in Eq. (11). It is true that the ac-dc correspondence could be fully predicted by the complex and more general separatrix crossing calculations of Cary, Chirikov, and Neishtadt,^{26–28} and so the calculation of the peak resonant impulse in Sec. II is included to demonstrate the dc limit in a more transparent manner for a simple but still very illuminating scenario.

Thus the ac-dc correspondence shown in this paper is robust and does not necessarily require potentials with fixed amplitude and constant acceleration. For instance, if the amplitude of the wave were held fixed and the phase velocity were varied monotonically, then a dc-like impulse still would be imparted to the distribution as the slowness parameter governing the rate of phase velocity modulation became infinitely small. If the amplitude were allowed to vary adiabatically, then some degree of compression and expansion of the distribution could occur as different parts of the distribution experience varying resonant interactions. However, the end result would still be an adiabatically displaced bulk distribution, perhaps stretched or compressed in velocity space, with tendrils of highly resonant phase space disappearing as the change in the time-varying parameters in the Hamiltonian becomes infinitely slow.

Other periodic potential configurations, such as an infinite train of widely spaced Gaussian wave packets, similarly result in the dc limit as long as the periodic structure is

accelerated adiabatically. This result suggests that a viable current drive scheme does not necessarily require an infinite sinusoidal beat wave or optical lattice; rather, an identical effect could be achieved using a series of pulsed, accelerating wave packets, each with some well-localized ponderomotive interaction range much smaller than the spacing between adjacent wave packet centroids.

IV. IMPORTANCE OF THE EFFECTIVE dc LIMIT

In acting like a dc field, the packets of ac fields acquire key properties of the dc field. For example, an important property of a dc electric field is that it accelerates all particles with uniform force regardless of the particle velocity. Because of this key property, the dc electric field can extract energy from particles that it slows down. This makes the dc field a very efficient generator of electric current; although it takes field energy to accelerate electrons to higher velocity, the energy flow is the opposite for electrons that are decelerated. In contrast, in wave-based acceleration schemes for producing current, which are based on wave-particle diffusion, the efficiency of current drive tends to be less to the extent that current is only produced as waves diffuse particles to higher energy.²⁹ If waves can only diffuse particles to higher energy, the opportunity to drive current by losing energy to the fields is absent, thereby diminishing the current drive efficiency.

There is an exception to this rule, but only a minor one: waves can diffuse particles to lower energy, but only when a population inversion exists along the diffusion path, such as in the presence of a density gradient.³⁰ However, such a situation requires not only density gradients, but also wave-particle diffusion paths that can exploit that gradient. Therefore, in general, the current drive efficiency by waves tends to be smaller than by a dc field.

To be specific, the total efficiency of generating current can be put as the ratio of the current generated to the power needed, J/P_{rf} . The power needed is just the rf power dissipated in the plasma, if all of the ac power is used. In general, however, there will be inefficiency in the use of this power, since some of this power will not be dissipated in the plasma and may not be easily recaptured and reused, which is discussed further below. Thus, defining the efficiency of generating current in terms of the ratio of the induced current density to the power dissipated in the plasma, J/P_D , then the total efficiency of the accelerating waves can be written as

$$\frac{J}{P_{\text{rf}}} = \eta \frac{J}{P_D}, \quad (14)$$

where $\eta \equiv P_D/P_{\text{rf}}$. Assuming dc-like displacement of the entire distribution such that the induced current density $J = ne\Delta v$, the fields driving the acceleration relinquish energy $|\Delta U_{\text{field}}| = nm(\Delta v)^2/2$ to the particles. Assuming an average 90° collisional frequency $\nu(v) \approx \nu_c$, the cost in power dissipated in the plasma in order to maintain the current is approximately $P_D \approx \nu_c |\Delta U_{\text{field}}|$. If the ratio $J/P_D = 2e/\nu_c m \Delta v \equiv 1/E_{\text{eff}}$, or in other words an effective dc electric field is defined, then $J = \sigma_{\text{Sp}} E_{\text{eff}}$, where $\sigma_{\text{Sp}} = 2ne^2/\nu_c m$ is just the Spitzer conductivity. This result leads to the expression

$$\frac{J}{P_D} = \frac{\sigma_{\text{Sp}}}{J}. \quad (15)$$

Thus the important conclusion is reached that for small current density, the efficiency scales inversely with J , making it much more efficient as $J \rightarrow 0$ than conventional rf techniques, where the efficiency does not vary with J . Collisional dissipation during a sweep through resonance is neglected, as it is assumed the sweeping occurs on a time scale $\Delta t \ll 1/\nu_c$. Since the oscillatory energy ϵ_{osc} is of the same order as the energy ϵ_f acquired by the particle following a full sweep, cf. Fig. 1, the constraint on Δt ensures that the rate of dissipation of oscillatory energy $\epsilon_{\text{osc}}\nu_c\Delta t \ll \epsilon_f$. The value of η in Eq. (14) depends on the specific implementation of the rf power and is strongly affected, for instance, by the ability to recirculate and reuse power that is not dissipated in the plasma on the first pass. The calculation of η is beyond the scope of the present work, but the optimization of the component of the efficiency going like J/P_D is clear nonetheless.

In addition to the exchange of energy between the potential packets and the particles, there could also then be an exchange of energy between the packets or a redshifting of the packets when the particles gain energy. From the standpoint of entropy production, the energy remaining in the packet can be fully convertible to do useful work, but the practical implementation of that conversion needs to be addressed. The calculation of η in Eq. (14) will also depend on these effects.

Making up in part for the inability of waves to produce current by extracting energy from countercurrent going electrons is the ability of waves to target specific populations of charged particles through wave-particle resonance conditions. For example, the ability to target specific populations allows waves to interact selectively with electrons or with one species of ions of a specific energy. Thus, the lower-hybrid current drive efficiencies³¹ or the electron cyclotron current drive efficiencies³² can be quite high by selective acceleration of low-collisionality electrons, namely, superthermal electrons. Nonetheless, while rf current drive schemes can be optimized by means of resonance conditions to have high efficiency, they still produce efficiencies not quite as high, in general, as for the Ohmic current drive obtained by a dc electric field, specifically in the limit as $J \rightarrow 0$, considering Eq. (15).

This feature of species discrimination by waves is notably retained even as energy discrimination is importantly lost. Referring to Eq. (9), note that $\epsilon \sim m$, and so while ϵ might be very small for electrons, ions encountering the same waveform might see a much larger ϵ . Although the analysis above focused mainly on the case of small ϵ , numerical simulations have demonstrated that as ϵ becomes of order one, the time-asymptotic impulse becomes highly sensitive to initial conditions, and as ϵ gets much larger than one, the impulse delivered to a particle becomes negligible.

Furthermore, the potential given in Eq. (1) can have an implicit mass dependency. In the absence of a magnetic field, the ponderomotive potential is given by

$$\Phi_P = \frac{e^2|E_0|^2}{4m\omega^2} \quad (16)$$

for an electric field with amplitude E_0 and characteristic frequency ω .³³ The inverse mass dependence of the magnitude of Φ_P suggests that electrons will experience a much stronger interaction with the optical lattice than the ion populations. However, in the presence of an approximately uniform, static magnetic field, the ponderomotive potential becomes

$$\Phi_P = \sum_{\nu} \frac{e^2|E_{\nu}|^2}{4m\omega(\omega - \nu\Omega)}, \quad (17)$$

where the sum is over the values $\nu = \pm 1, 0$, with $\nu = \pm 1$ corresponding to the left- and right-hand circularly polarized transverse electric field components, respectively, and $\nu = 0$ corresponding to the longitudinal electric field component.²³

In the case of longitudinal current drive, the dynamics is still approximately one-dimensional and the equation of motion used in Sec. II is unchanged. The presence of a resonant denominator in Eq. (17) suggests that it is possible in principle to calibrate ω near some Ω_s for a particular species s , ion or electron, such that s experiences a much larger response than all other species, allowing for the possibility of driving a single species in a dc-like manner while leaving all other populations virtually unchanged. However, Eq. (17) presumes the driven particle is far enough out of resonance for adiabatic analysis to hold; as the singularity at resonance is approached the particle dynamics becomes nonadiabatic, and the form of the ponderomotive potential changes,³⁴ so the strength of Φ_P cannot be increased without limit.

Thus, while the dc-like acceleration mechanism might not be able to target a specific part of a particle distribution, it *can* in principle discriminate between distributions corresponding to different particle species. Note also that the driving of one species is accomplished without increase in entropy of the driven species, as with a dc field, compared with ponderomotive one-way wall effects, which do increase the particle entropy.³⁵

However, even as the acceleration may be efficient, generating current through rf fields still retains the advantages of ac-like acceleration over acceleration with dc electric fields. Most importantly, a dc electric field driving a toroidal current has a nonvanishing curl, so there is necessarily a monotonically time-varying magnetic field, which means that the current cannot be sustained in a purely steady state. This restriction does not apply to rf waves, which can generate purely steady state currents, thus enabling, for example, purely steady state tokamak reactors producing nuclear fusion.

Note that the dc-like acceleration could be cycled indefinitely, allowing a distribution to be repeatedly kicked in the current-going direction. Multiple cycles within an electron collisional time could ramp up the current to incrementally higher levels without distorting the shape of the underlying distribution; thus, an initially Maxwellian distribution would remain a shifted Maxwellian, with all of the damped wave energy going into directed, and not thermal, motion. Even as different parts of the accelerated distribution relax collisionally at different rates, the amount of current generated by

each successive pulse remains constant, proportional only to the overall electron density, $J_{\text{tot}} \sim en_e \Delta \dot{x}$, with $\Delta \dot{x}$ fixed. Diffusion-based ac acceleration schemes would instead bear some proportionality to density and/or velocity-space gradients of the distribution, which are quantities that would not remain constant during collisional relaxation. One potential issue that could arise from the constancy of each successive impulse is the production of runaway populations in the high energy tail of an electron distribution, since relaxation rates are proportional to $1/v^3$, but such effects could be mitigated simply by reducing the number of cycles per collisional time.

Waves can also be brought to bear on a plasma through different technological means than can dc fields, with a compact or remote apparatus, which is a technological advantage. Thus, the possibility of using waves, which are not restricted to pulsed operation and utilize different power technology, to mimic the effects of dc fields could be, in principle, of considerable practical interest. There might be an opportunity to capitalize both on the high efficiency of dc-driven currents and the advantages of wave generation technology.

It is also curious that an exchange of wave packets mimics in this limit the effect of a dc field. Note that the wave packets forming the optical lattice behave in some ways like particles. These packets are localized and conserve photons (or the generalization of photons in the plasma medium). Thus, it takes counterpropagating wave packets to produce what acts essentially as a force field, at least in the limit identified here. It is worth noting that there is a structural resemblance between the use of packets to mediate fields here and say other particle exchanges that mediate force fields in quantum field theory.

V. CONCLUSIONS

What is shown here is that waves can induce populations of charged particles to behave like they do in dc fields, but only in certain limiting cases of slowly accelerating coherent wave structures. Moreover, the phase space conservation is very different on a fine scale, and only in an averaged sense do the two effects coincide. However, in the limit of slowly accelerating waves, the portion of phase space not obeying dc-like behavior becomes vanishingly small.

The bucket model for an adiabatically accelerating sinusoidal potential predicts that the resonant interaction with a waterbag distribution essentially displaces the boundaries of the distribution an equal amount in velocity space in order to accommodate the empty volume moved through the distribution by the time-asymptotically unfilled bound states of the system. This effect is confirmed by a more rigorous analysis of the peak resonant impulse delivered to particles throughout phase space, which shows that the parts of the distribution that are highly resonant with the wave and deviate substantially from the prediction established by the adiabatic jump condition disappear in the limit of slow acceleration. If the wave phase velocity is accelerated infinitely slowly, the time-asymptotic effect of the wave on the whole distribution scales exactly like the bucket displacement model predicts and is, in fact, indistinguishable from the effect of a uniform

dc field applied for a finite period of time. Previous works indicate that this effect is very robust and not simply limited to potentials accelerated at a constant rate.^{26–28}

The utility of ac fields for dc-like acceleration is that it can retain important features of wave-based methods for current drive and particle acceleration as well as important features of dc-field acceleration. The adiabatically accelerated wave method was noted to have the potential to exhibit near dc-like efficiency, since the wave both gives energy to particles going in the desired direction and takes energy from particles traveling in the other direction, exactly as a momentarily applied dc field would do. Additionally, this dc-like acceleration mechanism does not heat the distribution, allowing all expended wave energy to be applied to directed, and not thermal, motion. At the same time, there are opportunities for species selection, wave penetration, and quasisteady state operation with no loss of current production over many successive cycles.

Insofar as dissipation in the plasma is concerned, the high efficiency in accelerating a particle distribution during one cycle lends itself to sustained high efficiencies over many cycles. However, the full energy efficiency depends on whether the energy retrieved by the wave components of the accelerating potential from the parts of the particle distribution that slow down can be recycled in such a way as to make use of that recovered energy. The energy recovery will depend on the specific implementation of accelerating wave potentials.

Finally, it is an objective of this work to draw attention to the purely academic interest that such a correspondence between ac and dc fields could exist at all. Particularly in view of the natural implementation of this effect through counterpropagating wave packets, there appears to be more than a casual similarity to quantum field theory, where fundamental forces between particles can be described in terms of static force fields and exchanges of force carriers between the particles.

ACKNOWLEDGMENTS

The authors would like to thank Lazar Friedland, Pavel Khain, Jonathan Wurtele, and Ilya Dodin for useful discussions. This work was supported by U.S. DOE Contract No. DE-AC02-76-CH03073. One of us (P.F.S.) was supported by the National Defense Science and Engineering Graduate Fellowship.

APPENDIX: CALCULATION OF PEAK RESONANCE IMPULSE

The expression for $\Delta \dot{x}(\eta_i)$ shown in Eq. (11) can be derived as follows. Consider a general accelerating one-dimensional potential of the form $\phi[x - \psi(t)]$, with ψ an arbitrary function of time. An ideal reference frame in which to perform analysis would be the noninertial rest frame of the potential, whose coordinate is defined by $s \equiv x - \psi(t)$. In this coordinate system, the equation of motion becomes

$$m\ddot{x} = m(\ddot{s} + \ddot{\psi}) = -\frac{\partial\phi}{\partial x} = -\frac{\partial\phi}{\partial s}. \quad (\text{A1})$$

A conserved quasienergy E can be identified by multiplying Eq. (A1) by \dot{s} ,

$$\frac{d}{dt}\left(\frac{1}{2}m\dot{s}^2 + \phi(s) + m\dot{\psi}s\right) \equiv \frac{dE}{dt} = m\dot{s}\ddot{\psi}. \quad (\text{A2})$$

The term on the right-hand side of Eq. (A2) can be thought of as a driving term for the quasienergy, but in the case of a potential accelerating at the constant rate a , i.e., $\psi(t) = \frac{1}{2}at^2 + v_0t + x_0$, the quasienergy is conserved, since $\ddot{\psi} = 0$. Thus, the dynamics arising from the accelerating potential is taken into account by the introduction of an additional linear potential $m\dot{\psi}s = mas$ into the quasienergy in the frame of reference moving with the potential.

The impulse delivered to a classical particle by an accelerating potential is calculated as

$$\begin{aligned} \Delta\dot{x} &= \int_{t_i}^{t_f} \ddot{x} dt \\ &= \int_{t_i}^{t_f} (\ddot{s} + \ddot{\psi}) dt \\ &= \int_{t_i}^{t_f} \ddot{s} dt + \int_{s_i}^{s_f} \frac{\ddot{\psi}}{\dot{s}} ds = \dot{s}(t_f) - \dot{s}(t_i) + a \int_{s_i}^{s_f} \frac{ds}{\dot{s}}, \end{aligned}$$

where the coordinate representation $s \equiv x - (1/2at^2 + v_0t + x_0)$ is used for the constant acceleration case. $s(t_i) \equiv s_i$ and $s(t_f) \equiv s_f$ are both defined. In this reference frame, the quasienergy defined in Eq. (A2) is conserved, and so if $\dot{s}(t_i) = \dot{s}[s(t_i)] \equiv \dot{s}_i$ is specified by an initial condition, $\dot{s}(t_f) = \dot{s}[s(t_f)] \equiv \dot{s}_f$ can be determined immediately. To simplify notation, the quantity τ is defined as

$$\tau \equiv \int_{s_i}^{s_f} \frac{ds}{\dot{s}} + \frac{1}{a}(\dot{s}_f - \dot{s}_i) \quad (\text{A3})$$

with

$$\dot{s} = \left\{ \frac{2}{m}[E - \phi(s) - mas] \right\}^{1/2},$$

and E is the conserved quasienergy in the noninertial frame of reference. According to this definition,

$$\Delta\dot{x} = a\tau. \quad (\text{A4})$$

Time asymptotic impulses can be calculated by setting one bound of the integral at the classical turning point in the quasipotential and the other at the infinity toward which the potential becomes increasingly negative, due to the presence of the extra linear term, and multiplying the result by 2. This corresponds to the scenario where the wave starts with an infinite phase velocity in one direction and accelerates until it has an infinite phase velocity in the opposite direction.

Assuming $\epsilon > 0$, the time-asymptotic τ -integral for a particle in the quasipotential $f(\eta)$, defined in Eq. (8), is given by

$$\begin{aligned} \tau_\infty &= 2 \left(\int_{-\infty}^{\eta_t} \frac{d\eta}{\dot{\eta}} - \frac{|\dot{\eta}_{-\infty}|}{ka} \right) \\ &= 2^{1/2} \int_{-\infty}^{\eta_t} \frac{d\eta}{[E - f(\eta)]^{1/2}} - \frac{2|\dot{\eta}_{-\infty}|}{ka} \end{aligned} \quad (\text{A5})$$

with

$$\dot{\eta} = \{2[E - f(\eta)]\}^{1/2}. \quad (\text{A6})$$

Note that η_t signifies the phase of the classical turning point of the particle in the quasipotential, which itself depends on the relationship between the particle quasienergy E , $\tilde{\phi}$, and ϵ . This form of τ_∞ is justified by the observation from Eq. (A3) that the ‘‘uphill’’ and ‘‘downhill’’ components of τ_∞ will be symmetric and of the same sign. The integral in Eq. (A5) corresponds to the amount of time it takes the particle to move from minus infinity to the turning point or vice versa, and $|\dot{\eta}_{-\infty}|$ corresponds to the particle speed at minus infinity, all in the rest frame of the wave. This is an inconvenient form for τ_∞ , because the difference between two infinite quantities must be calculated to get a finite result. However, numerical simulations of particles interacting with an accelerating potential have shown that the majority of the net impulse delivered to the particle occurs during the peak fluctuation as the particle passes through exact wave-particle resonance; cf. Fig. 1. The particle is in exact resonance with the wave when it is traveling at the same instantaneous velocity as the wave, which corresponds to when the particle is at the classical turning point in the quasipotential picture.

Now postulate that the salient features of the time-asymptotic wave-particle interaction will be demonstrated in the peak resonant impulse delivered to the particle during the strongest part of the resonant interaction, i.e., the largest fluctuation depicted in Fig. 1. The most significant variations in the outcomes of different interactions should be determined by the particle dynamics very near the turning point in the quasipotential during this peak resonant fluctuation. On the other hand, the remainder of the interaction far from the turning point should not be strongly sensitive to the exact energy of the particle and could be time averaged. The peak resonant impulse can be calculated with the τ -integral

$$\tau_p = 2 \left[\int_{\eta_{\min}}^{\eta_t} \frac{d\eta}{\dot{\eta}} - \frac{\dot{\eta}(\eta_{\min})}{ka} \right], \quad (\text{A7})$$

where η_{\min} is the local minimum of $f(\eta)$ nearest the turning point, cf. Fig. 6. Specifically, looking ahead to Eq. (A8), for interval of validity \mathcal{D}_m , $\eta_{\min} = 2\pi m - \sin^{-1} \epsilon - \pi$.

τ_p is calculated for the accelerating sinusoidal quasipotential in Eq. (10) as follows. In order that a second order expansion of the cosine term in $f(\eta)$ will provide sufficient accuracy over the whole integration range, the integration can be split into two separate parts,

$$\tau_p = 2 \left[\left(\int_{\eta_{\min}}^{\eta_*} + \int_{\eta_*}^{\eta_t} \right) \frac{d\eta}{\dot{\eta}} - \frac{\dot{\eta}(\eta_{\min})}{\tilde{\phi}\epsilon} \right],$$

where $\eta_* = (\eta_t + \eta_{\min})/2$ and $ka = \tilde{\phi}\epsilon$. Now expand $f(\eta)$ to second order in η about η_{\min} for the first integral and about

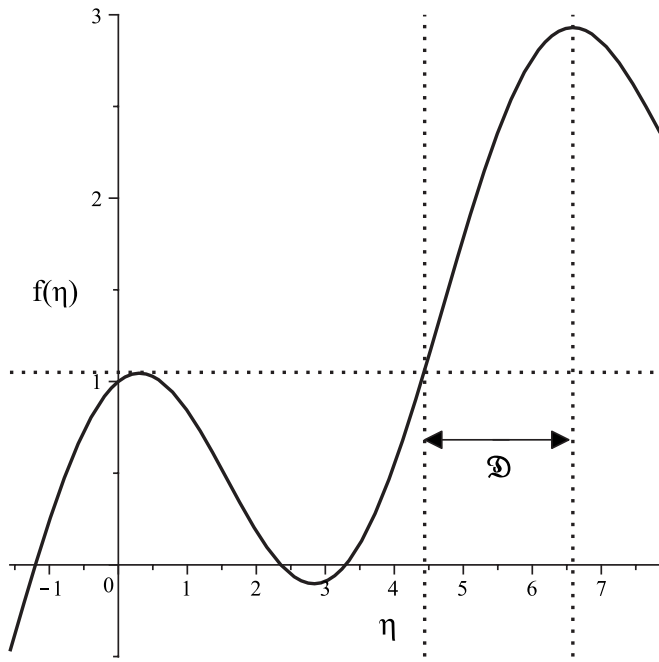


FIG. 6. Example interval of domain of validity \mathcal{D}_1 for Eq. (11), corresponding to $m=1$ in Eq. (A8).

η_t for the second integral. Define new integration variables $x \equiv \eta_t - \eta$ and $y \equiv \eta - \eta_{\min}$, at which point

$$\tau_p \approx 2 \left\{ \int_0^{\Theta(\eta_t)} \frac{dy}{[2(f(\eta_t) - f(\eta_{\min})) - f''(\eta_{\min})y^2]^{1/2}} + \int_0^{\Theta(\eta_t)} \frac{dx}{[2f'(\eta_t)x - f''(\eta_t)x^2]^{1/2}} - \frac{\dot{\eta}(\eta_{\min})}{\tilde{\phi}\epsilon} \right\},$$

where $\Theta(\eta_t) \equiv (\eta_t - \eta_{\min})/2$ and $E=f(\eta_t)$ was used. The equation for τ_p above is general for arbitrary quasipotential $f(\eta)$ and possesses an exact analytical solution that yields τ_p as a function of the classical turning point η_t . This form for τ_p leads to the expression for $\Delta\dot{x}(\eta_t)$ found in Eq. (11) for the sinusoidal quasipotential in Eq. (10).

The domain of validity \mathcal{D} of this expression for τ_p can be extended over a countably infinite number of discontinuous intervals in η , due to the fact that a particle must energetically climb higher up a wave crest in the quasipotential than the local maximum of the adjacent, lower wave crest in order for that point to represent a valid turning point; otherwise, the particle would have turned on the previous wave crest instead. Figure 6 illustrates this concept. An arbitrary interval of the domain of validity is calculated to be approximately

$$\mathcal{D}_m = (2\pi m + [\epsilon - \{\epsilon^2 + 2[1 - \sqrt{1 - \epsilon^2}] + \epsilon(2\pi - \arcsin \epsilon)\}^{1/2}], \arcsin \epsilon + 2\pi m), \quad (\text{A8})$$

with m any integer; for instance, the representation given in Eq. (11) is valid over the domain \mathcal{D}_0 . The limit where the wave acceleration approaches zero is of particular interest, i.e., $\epsilon \rightarrow 0$. Referring to Eq. (A8), the interval \mathcal{D}_0 goes like

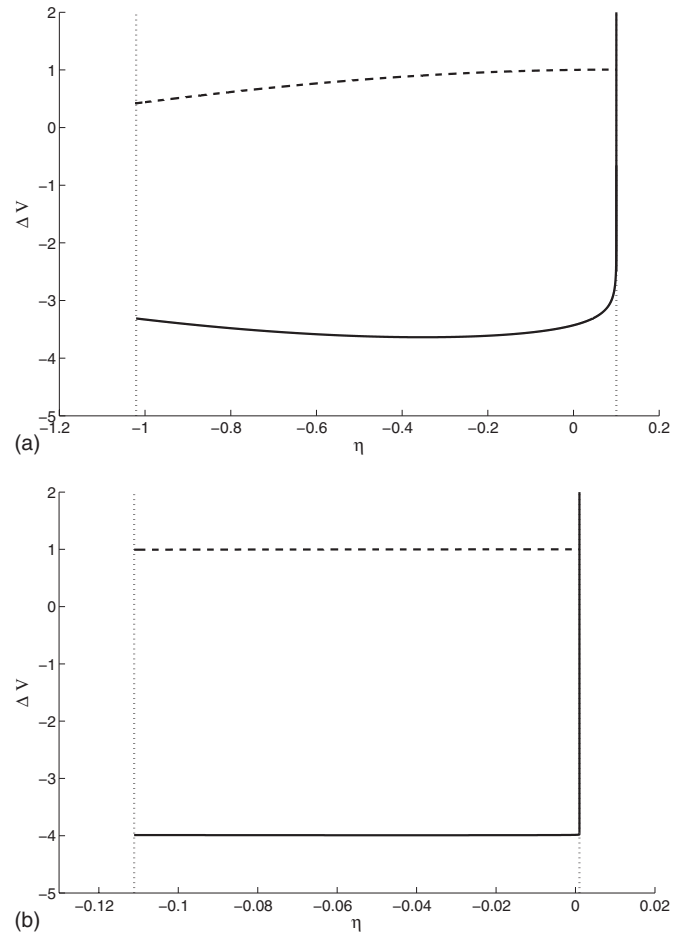


FIG. 7. Analytic approximation for $\Delta\dot{x}(\eta)=a\tau_p(\eta)$ [solid line, cf. Eqs. (A4) and (11)] plotted against the quasipotential $f(\eta)$ [dashed line, cf. Eq. (10)] over the domain corresponding to $m=0$ in Eq. (A8) for (a) $\epsilon=10^{-1}$ and (b) $\epsilon=10^{-3}$. Limits η_{\min} and η_{\max} are traced out by dotted lines.

$$\mathcal{D}_0 \approx (\epsilon - (4\pi\epsilon)^{1/2}, \epsilon]. \quad (\text{A9})$$

Using Eqs. (A4) and (9), $\Delta\dot{x}_p$ becomes

$$\Delta\dot{x}_p = a\tau_p = \frac{\epsilon\tilde{\phi}}{k}\tau_p. \quad (\text{A10})$$

Since Eq. (A9) states that over the valid domain for Eq. (A10), the value of $\eta_t \ll 1$, Eq. (11) can be expanded for small ϵ and small η_t , and this leads eventually to the form of $\Delta\dot{x}(\eta_t)$ shown in Eq. (12).

Figure 7 illustrates the behavior of $\Delta\dot{x}_p(\eta_t)=a\tau_p(\eta_t)$ over three orders of magnitude in ϵ . The right limit of the domain marks the location of η_{crit} , the point of unstable equilibrium in the quasipotential. Note that while the singularity in the impulse is pronounced for $\epsilon=10^{-1}$, its presence is limited to an almost trivial fraction of the domain when $\epsilon=10^{-3}$, so small that it would not plot and had to be represented graphically using manual input of a vertical line at η_{crit} . On the other hand, the ‘‘bulk’’ behavior makes a smooth transition to a nearly flat, adiabatic response as ϵ is decreased.

- ¹L. Friedland, P. Khain, and A. G. Shagalov, *Phys. Rev. Lett.* **96**, 225001 (2006).
- ²P. Khain and L. Friedland, *Phys. Plasmas* **14**, 082110 (2007).
- ³A. M. Sessler and K. R. Symon, Proceedings of the CERN Symposium on High Energy Accelerator, Geneva, 1956 (unpublished), p. 44.
- ⁴A. Hofmann, "Design and utilization of the SSC summer study," Report No. SLAC-PUB-3427, 1984.
- ⁵N. M. Kroll, P. L. Morton, and M. N. Rosenbluth, *IEEE J. Quantum Electron.* **17**, 1436 (1981).
- ⁶F. Peinetti, W. Bertsche, J. Fajans, J. Wurtele, and L. Friedland, *Phys. Plasmas* **12**, 062112 (2005).
- ⁷L. Friedland, F. Peinetti, W. Bertsche, J. Fajans, and J. Wurtele, *Phys. Plasmas* **11**, 4305 (2004).
- ⁸W. Bertsche, J. Fajans, and L. Friedland, *Phys. Rev. Lett.* **91**, 265003 (2003).
- ⁹M. N. Schneider, P. F. Barker, and S. F. Gimelshein, *Appl. Phys. A: Mater. Sci. Process.* **89**, 337 (2007).
- ¹⁰S. X. Hu and A. F. Starace, *Phys. Rev. Lett.* **88**, 245003 (2002).
- ¹¹I. Y. Dodin and N. J. Fisch, *Phys. Rev. E* **68**, 056402 (2003).
- ¹²K. P. Singh and H. K. Malik, *Appl. Phys. Lett.* **93**, 044101 (2008).
- ¹³D. L. Bruhwiler and J. R. Cary, *Phys. Rev. Lett.* **68**, 255 (1992).
- ¹⁴D. L. Bruhwiler and J. R. Cary, *Phys. Rev. E* **50**, 3949 (1994).
- ¹⁵L. Feng and Y. Ho, *Phys. Rev. E* **47**, R2277 (1993).
- ¹⁶L. Cicchitelli and H. Hora, *IEEE J. Quantum Electron.* **26**, 1833 (1990).
- ¹⁷J. X. Wang, Y. K. Ho, L. Feng, Q. Kong, P. X. Wang, Z. S. Yuan, and W. Scheid, *Phys. Rev. E* **60**, 7473 (1999).
- ¹⁸G. Shvets, N. J. Fisch, and A. Pukhov, *IEEE Trans. Plasma Sci.* **28**, 1194 (2000).
- ¹⁹R. R. Lindberg, A. E. Charman, J. S. Wurtele, and L. Friedland, *Phys. Rev. Lett.* **93**, 055001 (2004).
- ²⁰D. N. Gupta and H. Suk, *Phys. Plasmas* **13**, 013105 (2006).
- ²¹I. Y. Dodin and N. J. Fisch, *Phys. Rev. E* **72**, 046602 (2005).
- ²²I. Y. Dodin, N. J. Fisch, and J. M. Rax, *Phys. Plasmas* **11**, 5046 (2004).
- ²³H. Motz and C. J. H. Watson, *Adv. Electron.* **23**, 153 (1967).
- ²⁴E. Esarey, P. Sprangle, J. Krall, and A. Ting, *IEEE Trans. Plasma Sci.* **24**, 252 (1996).
- ²⁵I. Y. Dodin and N. J. Fisch, *Phys. Plasmas* **15**, 103105 (2008).
- ²⁶B. V. Chirikov, *Dokl. Akad. Nauk SSSR* **125**, 1015 (1959).
- ²⁷J. R. Cary, D. F. Escande, and J. L. Tennyson, *Phys. Rev. A* **34**, 4256 (1986).
- ²⁸A. I. Neishtadt, *Prikl. Mat. Mekh.* **51**, 586 (1987).
- ²⁹N. J. Fisch, *Rev. Mod. Phys.* **59**, 175 (1987).
- ³⁰N. J. Fisch and J. M. Rax, *Phys. Rev. Lett.* **69**, 612 (1992).
- ³¹N. J. Fisch, *Phys. Rev. Lett.* **41**, 873 (1978).
- ³²N. J. Fisch and A. H. Boozer, *Phys. Rev. Lett.* **45**, 720 (1980).
- ³³A. V. Gaponov and M. A. Miller, *Sov. Phys. JETP* **7**, 515 (1958).
- ³⁴I. Y. Dodin and N. J. Fisch, *Phys. Lett. A* **349**, 356 (2006).
- ³⁵N. J. Fisch, J. M. Rax, and I. Y. Dodin, *Phys. Rev. Lett.* **91**, 205004 (2003).